75th International Astronautical Congress (IAC), Milan, Italy, 14-18 October 2024.

IAC–24–B2.4.8

End-to-End Availability Analysis for an Optical-RF Large Constellation Concept

Samuele Raffa*, Luca Pizzuto, Juraj Poliak
German Aerospace Center - Institute of Communications and Navigation, Germany
*Corresponding Author, samuele.raffa@dlr.de

Optical Satellite Links (OSL) are increasingly popular, due to their undisputed advantages with respect to standard radio communications in terms of achievable bandwidth and virtually non-existent band interference issues. Several Large Constellations that are currently operating or being designed foresee the use of OSL, at the very least, for the Inter-Satellite Link segments. As for the optical Feeder-Link part, cloud blockage still poses a considerable availability limitation factor. For this reason, multiple Optical Ground Stations (OGS) are needed to allow for site diversity, thus increasing link availability to the satellite constellation. We present a study on the coverage and access availability performance of two LEO constellation design options that use Optical (Uplink) Feeder-Links and Optical Inter-Satellite Links (OISL), while keeping an RF-based User Downlink. We then present the main results of the End-to-End (Ground-to-User) access availability, targeting Users in the European region. Furthermore, the performance increase on coverage and availability when implementing OISL in the communications architecture is discussed. The main focus is posed on the logic and implementation of a Python-based Network Optimisation Algorithm. The tool significantly improves the analysed availability results by identifying the optimal OGS network to guarantee User access availabilities above 99% with the least number of OGSs possible. User links have been modelled as a target grid across the European region. The Optimisation Algorithm is able to discriminate targets based on their priority ranking. One of the significant results was that a high-altitude low-density constellation needs significantly less OGSs than a low-altitude high-density constellation to reach an optimal User coverage and User access availability for the most important targets.

1 Introduction

Free Space Optical Communications (FSOC) between satellites and ground stations is a novel topic that is gaining more and more popularity, due to its possible advantages with respect to standard radio frequency communications. The benefits of optical communications technologies, mostly laid out in [1], include a higher bandwidth, lower power and mass requirements, high security and the absence of spectrum licensing. However, there are challenges associated with the higher frequency deployed, mostly the presence of clouds and turbulence from the atmosphere, which may block any optical uplink or downlink to and from the satellites. Researchers are actively working to find optimal solutions to these challenges, with the goal of satisfying the increasing demands for high data rate and low latency communications by designing satellite constellations that include optical links.

Since the pioneering theoretical study on optical transmission from ground to space [2], numerous theoretical investigations and successful experiments have been conducted to explore optical ground-to-satellite and inter-satellite communications technologies. Some of the most remarkable achievements include the Galileo optical experiment (GOPEX) in 1992, which demonstrated an optical uplink to a deep space vehicle [3]; the first ground-to-space two way communications link, in 1995 in the frame of the Ground/Orbiter Lasercom Demonstration (GOLD) [4], [5]. The first inter-satellite laser communications link was successfully demonstrated by ESA between the two satellites SPOT-4 and ARTEMIS for optical data-relay services at 50 Mbps [6]. More recently, a NASA mission, the Laser Communications Relay Demonstration (LCRD), was launched in 2017. This mission showcased the potential of optical relay services for both near Earth and deep space communications missions [7]. Another notable example of this technology is the European Data Relay System (EDRS) developed by the German Aerospace Center. The EDRS utilizes GEO satellites as relays to LEO satellites, primarily for commercial and disaster prevention purposes [8]. Along with FSOC, in the recent years the new-space telecommunications indus-

try showed a significant interest toward the concept of satellite constellations. A satellite constellation is a group of satellites, typically placed in sets of complementary orbital planes, working together as a system to achieve a unique objective. Constellations are generally used to fulfill spatial and temporal coverage requirements which cannot be met with a single satellite. Planned and existing new-space communications constellations are connected via RF-links to globally distributed ground stations, and they typically employ RF-based or optical-based inter-satellite links [9]. Our work adds to the previous research by proposing a new concept for use of existing RF infrastructure, boosted by upcoming optical communications solutions for Feeder-link and OISL on large LEO constellations. The main focus in this paper is posed on the logic and implementation of a Python-based Network Optimisation Algorithm. The tool significantly improves the analysed availability results, by identifying the optimal OGS network to guarantee optimal User Access availabilities with the least number of OGSs possible. User links have been modelled as a target grid across the European region. The Optimisation Algorithm is able to discriminate targets based on their priority ranking. After this introduction, the remainder of the paper is structured in four sections. In Section 2, the methodology for the simulaton and the analysis of the End-to-End Chain Access is presented, and in Section 3 the results for the basic configurations of constellations, ground stations and OISL options are shown. In Section 4 the concept of OGS Network Optimisation is introduced, aiming to achieve a good End-to-End User availability with an efficient use of the OGS Network. Results using this approach are also presented. In Section 5 the main conclusions of the work are derived, and the possible future works are discussed.

2 Methodology

In this analysis frame, two LEO satellite constellations (Walker-Delta type) have been considered, here named Constellation A and Constellation B. These two constellations represent a different approach to the design of constellation missions, with a trade-off between satellite density and orbit altitude. While lower orbits are easier to access, their reduced swath and coverage persistence shall require more satellites to provide homogeneous coverage. The features of the two satellite networks are summarized in table 1. These two constellation options share nevertheless the communications concept: the communications relay envisions an optical, high-throughput uplink where the aggregated data are sent from an optical ground station to the satellite node; from here, an RF-based downlink distributes the data to the ground users. To extend the relay range and area, a high-throughput OISL can be implemented. In this way, even if the optical uplink can connect to a single satellite node, the OISL connections would allow to distribute the data from other satellite nodes, potentially increasing the service availability. Visualisation of the communications concept is depicted in figure 1.

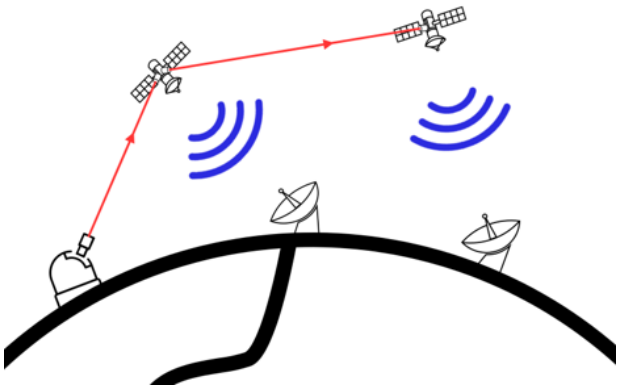

Fig. 1: Communications concept for the End-to-End (E2E) link. The red solid lines mark the Optical Links, the blue waves the RF Links.

As can be seen, each constellation has two possible data rates; the two values indicate the presence or not of OISL links. If the OISL is implemented, the OGSL data rate can then scale up, leveraging on the optical Feeder-link channel capacity and on the fact that, in this configuration, relay to ground user terminals will be performed by multiple satellite nodes via RF. In terms of constellation coverage analysis, the area of interest is the European area, defined simply as a rectangle, divided into 64 sub-targets, as it can be seen from figure 2.

2.1 *OGS Network*

It is generally assumed that the optical communications systems cannot penetrate clouds. Therefore, a collection of OGS locations and a database containing the 'clouds visibility predictions' for each specific OGS location must be adopted. For this analysis, 24 OGS locations were chosen across Europe according to good access to high-speed ground network, site diversity and acceptable proximity w.r.t. COLT Network points of presence [10]. The only exceptions are Athens and Catania, locations chosen due to good

Table 1: Constellations Characteristics. OGSL refers to Optical Ground-to-Space Link.

Parameter	Constellation A	Constellation B
Link type	OGSL	
Data rate [Gbps]	25-100	6-24
Altitude [km]	1200	500
Inclination [deg]	60	70
No. Planes	24	48
Satellites per Plane	12	24
Total Satellites	288	1152
Mean Link Duration [s]	397	169
Round-Trip Latency at Zenith [ms]	8.0	3.3

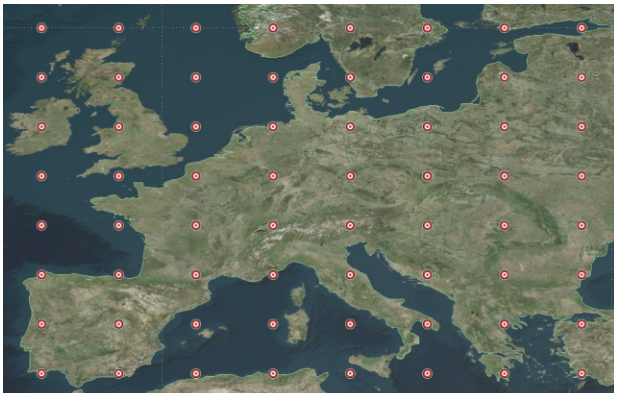

Fig. 2: Europe target grid divided into 64 targets.

Fig. 3: Locations of the 24 selected OGS.

clear-sky availability. The selected OGSs can be seen, over the European map, in figure 3. The database used to evaluate the sky availability of each OGS contains data retrieved and distributed by the University of Lille, showing the time windows in which the level of clearness of the sky is above a specific threshold. The threshold values were established on the basis of the previous ESA projects ONUBLA and ONUBLA+ [11]; considering a scale from 1 (best conditions, cloud-free) to 4 (worst conditions, blocking clouds), if the mask value is below or equal to 2, the optical link can potentially be established. Eventually, the advantage of a distributed OGS network is two-fold; for enhanced spatial access of a large target area, such as our study scenario, and for a better weather diversity and decorrelation, to increase the chances to have at least one of the OGS with clear line of sight to the space segment. At first, the 24 OGS locations have been organized in 8 networks of 5 OGSs each. These logical groupings were designed to predominantly allocate OGSs towards specific European regions. For instance, in the Southern configuration, all OGSs are positioned in southern Europe, whereas in the Central configuration, the OGSs are selected from central Europe. Additionally, the Best Cloud and Best Cloud per Quadrant (or Best Quadrant) networks select OGSs based on meteorological conditions rather than geographical locations. However, it is observed that the sky generally becomes clearer as one moves towards southern Europe, leading these last two networks to predominantly select OGSs located at lower latitudes in Europe. The OGS networks are presented in table 2.

2.2 *Link Topology*

For each of the two constellations, OISL capability was investigated, to understand what is the potential gain in terms of End-to-End availability on ground,

Table 2: OGS Networks composition.

Network Name	OGS in the Network
Best Cloud	Catania, Sevilla, Lisbon, Athens, Porto.
Best Cloud per Quadrant	Catania, Sevilla, Copenhagen, Paris, Marseille.
Northern	London, Dublin, Amsterdam, Copenhagen, Stockholm.
Southern	Lisbon, Barcelona, Catania, Athens, Rome.
Western	Dublin, Porto, London, Bordeaux, Barcelona.
Eastern	Athens, Sofia, Warsaw, Stockholm, Zagreb.
Central 1	Marseille, Milan, Paris, Vienna, Amsterdam.
Central 2	Geneva, Munich, Zagreb, Berlin, Marseille.

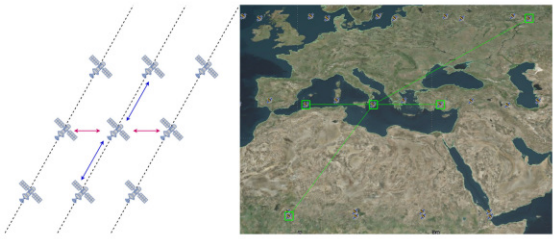

Fig. 4: Topology of 1 hop OISL. The central satellite (here visualized over south Italy) receives the uplink and connects with the four satellites of its hop.

when enabling satellite hops. The OISL considered are divided in two groups: intra-planar and inter-planar. Intra-planar links are performed between satellites on the same plane, namely between the central satellite and its leading and following ones. The quasi-constant range allows to consider these links as static. Inter-planar links are performed between satellites on different planes, namely between the central satellite and its two adjacent twins. These links are much more dynamic since the range changes significantly, but they are always visible to the central satellite, and at a shorter range than the intra-planar links. The topology of a single-hop OISL is showed in figure 4.

2.3 *Analysis Blueprint*

In the context of our analysis, an "access" refers to a temporal window during which a seamless connection can be established between the OGS, the satellite constellation, and the specific ground target. This necessitates the identification of overlaps between the uplink and downlink timeframes, which correspond to signals traveling from the OGS to the satellite and from the satellite to the target area, respectively. Each uplink segment must adhere to specific criteria. Firstly, the satellite must maintain a minimum elevation angle of 30 degrees relative to the OGS to ensure optimal signal geometry and minimize atmospheric attenuation effects. Secondly, the visibility conditions at the OGS site must be clear throughout the access period, as cloudy skies practically block the transmission of optical signals. These constraints are integral to FSO communications, where a high elevation angle is crucial for maximizing signal strength and reducing atmospheric interference, and clear weather conditions are essential to prevent signal degradation. For the downlink segment, which employs RF-based technology, only the topological constraint applies. Specifically, the satellite must be positioned at a minimum elevation angle of 25 degrees to facilitate effective communication with the ground target. This requirement ensures sufficient signal strength and quality for reliable data transfer to the designated area. Figure 5 illustrates the conceptual framework of this access chain and highlights the critical access window.

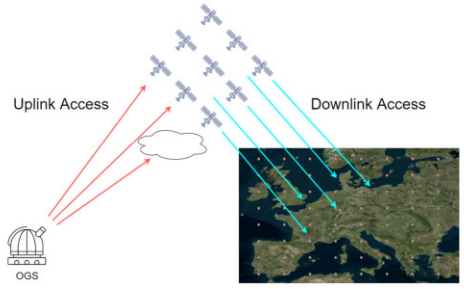

Fig. 5: Basic representation of the concept of Chain Access.

The preprocessing of the data was conducted using the AGI System Tool Kit (STK) software. This software facilitates the simulation of constellation networks, the propagation of satellite orbits, and the

generation of access reports. Through STK, we obtained the uplink databases for all 24 OGSs, detailing the access times of each OGS to the satellites in the constellation. Similarly, we obtained the downlink databases, which contain the access times of the satellites to the various targets. Given the quasi-periodic nature of the satellite orbits, these files were generated for a specific period, defined as the interval during which a satellite's ground track repeats. This corresponds to almost 8 days of propagation for constellation A and almost 17 days for constellation B. To extend the simulation to a full year, the geometric databases were replicated during post-processing. While this method introduces certain limitations and uncertainties, particularly over the long term, it strikes a balance between analytical precision and computational efficiency. The data for each period was replicated to simulate the satellite orbits over a year, a technique that, despite its challenges, was deemed the most effective given the constraints. Post-processing was performed using Python, with the databases managed by the Pandas library. Tasks were parallelized across the machine's cores using Python's built-in multiprocessing library. Each OGS underwent a chain analysis, which involved the computation of all possible accesses for a specific OGS, taking into account the topological and cloud-free requirements for the uplink and the topological requirement downlink segments. The output of the analysis is a chain database that, along with the chain databases of the other OGS in the network, is the building block of the network database. A valuable access will form a chain only if the full link between OGS, SAT and Ground Target is available. The entire chain generation process is shown in figure 6. The chain analysis was performed by breaking up the chain in two segments: OGS-to-SAT segment (Uplink segment) and SAT-to-Target segment (Downlink segment). The final database is then produced after having cross-checked the two segments data to find the time overlap between uplink and downlink that share the same satellite, which represents the central node of the chain. To obtain the final Chain database two filtering processes are required: cloud filtering and downlink filtering. The filtering process is translated into a simple query that merges two databases into a single one, selecting the regions where a temporal overlap is present. In the case of the cloud filtering, what we are looking for is the overlap between the uplink from a specific OGS and a condition of clear sky above the same OGS. The output of this process is a cloud filtered uplink database for each OGS, which will be used for the rest of the analysis and will be simply referred as 'Uplink database'. Once the chain databases for all the OGSs have been created, the final part of the analysis is the computation of the access availability of each network of OGSs. The end result is the Access Availability map of the network, which quantifies, for each target, the percentage of the simulation time during which at least one active chain access is available. In this study a so called Feederlink HandOver (FHO) is introduced, meaning that the OGS will connect to a rising satellite before the setting satellite moves outside of the visibility window, guaranteeing continuity in the communications between the OGS and the satellites of the constellation. This FHO technique is made possible by the significant density of the constellations, enabling every OGS to have always at least another available satellite when the current one is no longer visible.

3 OGS Network Configuration

All the results presented are based on the Chain databases computed assuming the previously explained FHO logic. Figure 7 shows the access availability for the "Best Cloud" network in constellation A.

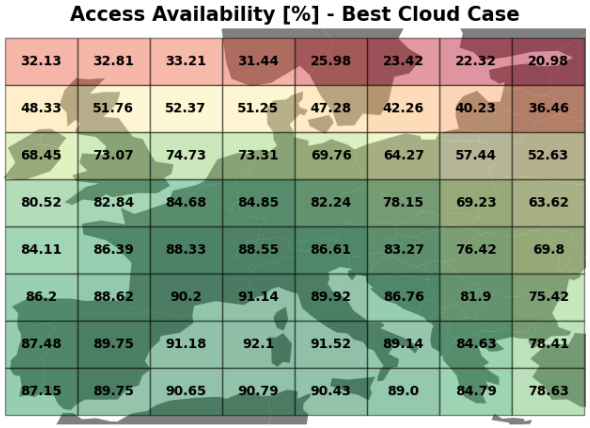

Fig. 7: Access Availability map for the Best Cloud network in constellation A.

These OGSs are all located in the south of Europe, hence the higher availability at the lower latitudes. We can see that, due to topological constraints, the higher latitudes are not sufficiently covered with this network configuration. Indeed, the majority of the total access time is concentrated in the south western areas of Europe, where the availability percent-

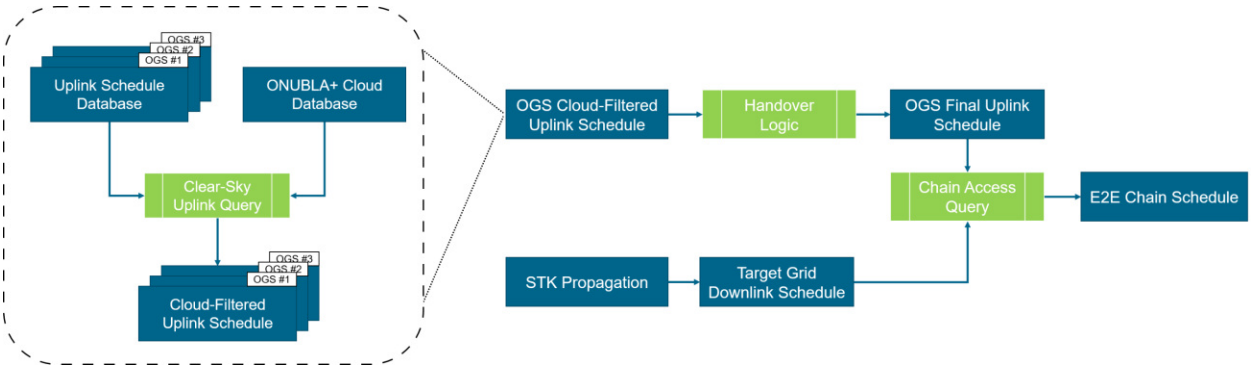

Fig. 6: Chain Access generation process.

ages are higher, while the north-eastern areas of Europe have less total access time, as highlighted by the smaller availability values. Figures 8 and 9 show the access availability map respectively for the "Best Cloud" and the "Western" networks, in constellation B.

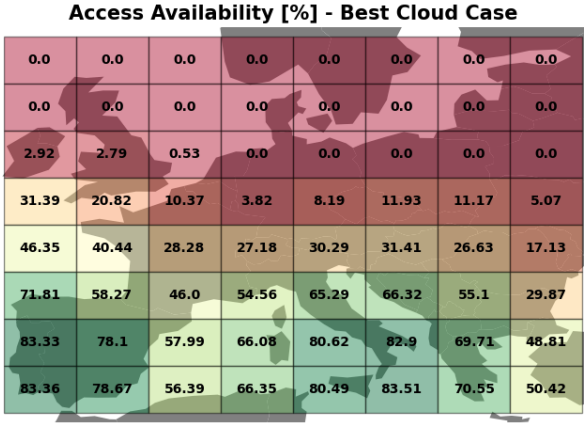

Fig. 8: Access Availability map for the Best Cloud Network in constellation B.

By looking at these two plots it emerges clearly the difference in the coverage and availability percentages: they both perform well for the south-western targets, but the Best Cloud has availability holes in the northern part of Europe while the Western in the eastern part of Europe, as expected looking at their OGSs distribution. Furthermore, a comparison between the Best Cloud network in Constellation A and its counterpart in Constellation B reveals superior coverage and availability metrics for the former. This enhanced performance can be attributed to the broader visibility cones of satellites in Constellation A, facilitated by their higher orbital altitude.

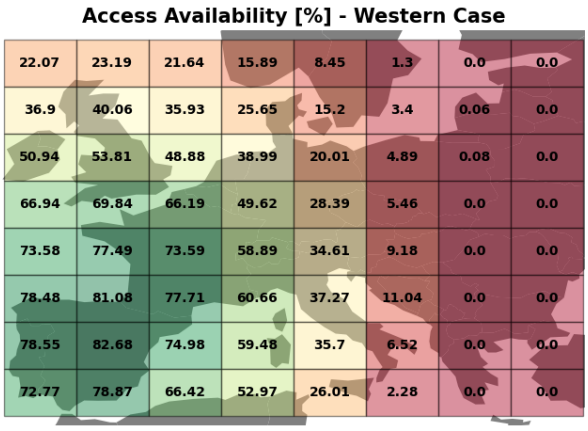

Fig. 9: Access Availability map for the Western Network in constellation B.

Such altitude enables these satellites to simultaneously be visible by multiple targets, even those situated at greater distances from the OGS transmitting the uplink signal. This advantage is particularly pronounced in the network's weaker areas, underscoring the critical role of orbital altitude in optimizing satellite network performance.

When introducing OISLs, satellite coverage drastically increases, enhancing the E2E availability. As an example, figure 10(a) shows the access availability map of the Best Cloud network after the introduction of OISL, in constellation A. We can see that the introduction of OISL does not add much to the southern area, where this network guarantees a good availability by definition, but significantly increases the performance in the northern area. In figure 10(b) it is shown the percentage improvement per target due to the introduction of OISL to the same network, computed as the difference between the availability

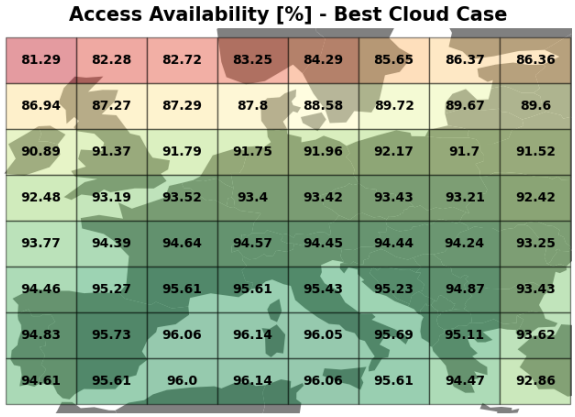

(a) Access Availability map with FHO and OISL.

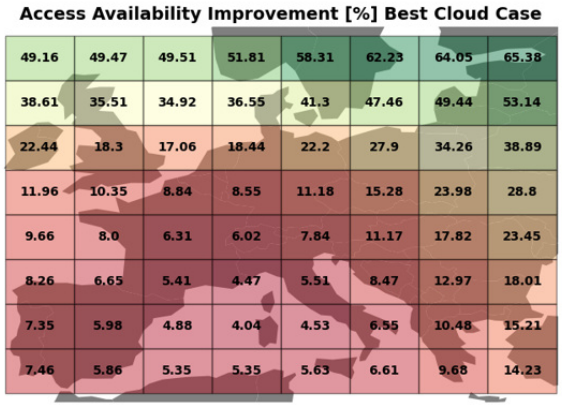

(b) Access Availability Improvement.

Fig. 10: Access Availability map (a) and improvement due to the introduction of OISL (b) for the Best Cloud Network in constellation A, with FHO and OISL.

after and before the introduction of the links. In figure 11(a) we can see the constellation B case, when adding OISL. Here we appreciate that the Northern area moves from a general absence of coverage to availability values between 30% and 78%, as shown by figure 11(b).

In Table 3 and 4 a summary of performances for different Link Configurations is presented, for the two distinct Constellations and the eight Ground Networks. Column "Uplink-only" refers to the uplink availability of the Network to the satellite segment, and it is exclusively driven by link topology and clear-sky access of the ground locations, representing the upper boundary of any achievable chain access availability. The other three columns present results for the chain access availability of the target grid. The three columns are defined by two description lines. First description line will read either "No OISL" or "OISL", indicating whether the satellite node, object of the Uplink, is capable of distributing the chain to the adjacent satellites. Second description line will read either "All Uplinks" or "Handover Logic". "All Uplinks" assumes no limitations to the number of Uplinks (i.e., number of satellites connected) to a single OGS. "Handover Logic" assumes a more realistic scenario, where the OGS will have only a single active uplink for most of the time, with only a second uplink active during handover, to guarantee continuous uplink operation when allowed by the conditions.

From the OISL implementation in the chain, the following conclusions can be drawn. Firstly, the comparative analysis between Constellation B and Constellation A underscores the latter's superior availability and coverage performance, consistent with prior topological and FHO results. Secondly, the OISL implementation significantly enhances access availability across the network, notably benefiting Constellation B, and introduces a decoupling between the physical location of the OGSs and individual target availability scores. Lastly, among the eight networks evaluated, those exhibiting more favorable atmospheric conditions—namely, the Best Cloud, Best Cloud per Quadrant, and Southern networks—outperform others. This outcome is anticipated, given that improved sky conditions facilitate a greater number of uplinks throughout the simulation period, thereby increasing chain access opportunities. It emerges that networks of 5 OGS are not sufficient to properly cover the targets and reach availabilities close to 100 %. The next step of the analysis is then to find out the minimum number of OGSs needed to reach availability percentages above 99 %, which is taken as a reference value, and to optimise the network to guarantee the best performance. To find these answers, a Network Optimisation (NO) tool was implemented.

4 Network Optimisation

The Network Optimization tool is built upon several key principles. First, a scoring system evaluates network performance through three sub-scores: availability, average chain duration, and availability homogeneity. The final score is a weighted mean of these sub-scores, ranging between 0 and 1.

Given the paramount importance of access availability, its score carries the highest weight, followed

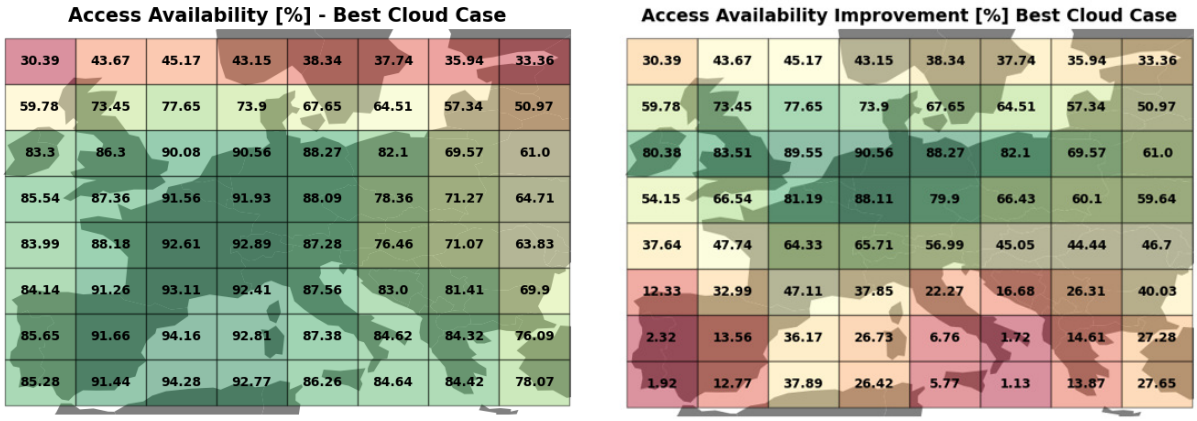

(a) Access Availability map with FHO and OISL.

(b) Access Availability Improvement.

Fig. 11: Access Availability map (a) and improvement due to the introduction of OISL (b) for the Best Cloud Network in constellation B, with FHO and OISL.

Table 3: Performance Metrics for Network CON A

Network ID	Uplink-only [%]	No OISL All Uplinks [%]	No OISL Handover Logic [%]	OISL Handover Logic [%]
Best Cloud	96.17	31.18 – 96.17	20.98 – 92.10	81.29 – 96.14
Best Quadrant	96.16	79.69 – 96.16	50.88 – 91.20	83.39 – 94.74
Northern	78.62	38.30 – 78.62	11.12 – 76.30	46.40 – 78.62
Southern	97.30	56.14 – 97.30	32.33 – 94.08	80.90 – 96.97
Eastern	87.90	47.25 – 87.90	16.75 – 84.36	72.61 – 86.75
Western	90.98	54.48 – 90.98	18.63 – 89.51	76.70 – 90.69
Central #1	84.80	80.57 – 84.80	40.68 – 83.98	74.27 – 84.78
Central #2	82.58	80.63 – 82.58	42.10 – 81.83	73.12 – 82.56

Table 4: Performance Metrics for Network CON B

Network ID	Uplink-only [%]	No OISL All Uplinks [%]	No OISL Handover Logic [%]	OISL Handover Logic [%]
Best Cloud	89.84	00.00 – 88.14	00.00 – 83.36	30.39 – 92.89
Best Quadrant	94.13	16.21 – 90.44	02.97 – 82.09	47.51 – 94.32
Northern	78.62	00.00 – 78.50	00.00 – 63.98	15.03 – 75.68
Southern	97.28	00.00 – 92.91	00.00 – 90.74	51.60 – 94.79
Eastern	87.11	00.00 – 79.21	00.00 – 76.46	01.32 – 82.37
Western	89.31	00.00 – 88.75	00.00 – 82.68	00.40 – 88.66
Central #1	84.80	01.30 – 84.43	00.24 – 80.67	25.30 – 83.99
Central #2	82.58	80.65 – 82.58	00.49 – 77.53	40.84 – 81.75

by the homogeneity score and then the duration score. Second, the combinatorial explosion in potential OGS configurations necessitates constraints such as minimum distances between OGSs. As a reference, the total number of possible combinations without repetition for 24 possible OGSs in groups of 5 equals to 42504, while for 10 OGSs it reaches the value of 1961256. Ensuring a minimum separation of 300 km between the OGSs helps avoid redundant or suboptimal network configurations. Third, target weights

are assigned based on the population density and significance of the target areas. This approach aids in differentiating between networks that appear to perform similarly overall. A qualitative priority target map is shown in figure 12.

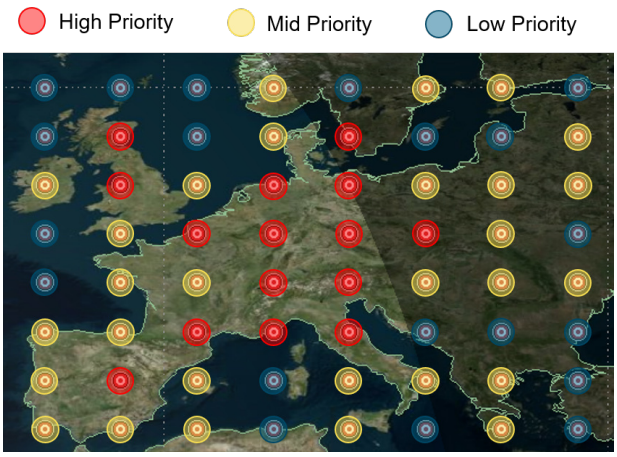

Fig. 12: Priority map of the targets used by the NO tool.

Fourth, efficiency is achieved by precomputing the uptime of each OGS, which is then stored and reused across different network evaluations. This method significantly reduces computation time when testing larger networks by performing the most time consuming computations only once per OGS. Finally, a trade-off mechanism identifies the top 10 networks based on overall and availability scores, while also suggesting potential improvements. This mechanism analyzes targets with lower availability, recommending additional OGSs to enhance network performance.

Table 5 shows the number of networks tested by the tool per each OGS number and constellation. In general, the number of networks tested is lower for constellation B than for constellation A, since the analysis of constellation B requires more time. For this reason, it was decided to scale the network size by adding only the OGSs that were selected by the tool as best candidates to decrease the outage times of the targets, instead of testing all the possible combinations. For constellation A the analysis was stopped at 11 OGSs, since that number of OGSs has shown to be sufficient to reach an optimal performance, reaching at least 99% on all the priority targets.

Table 6 shows the OGSs that make the best networks for a given number of OGSs. It is immediately visible how the majority of the OGSs are located at the lower latitudes, and some OGSs, like Catania and Marseille, are present in all the most performing networks.

Table 5: Number of networks tested per OGS number and Constellation.

OGS number	A - Classic	B - Classic
5	370	389
6	131	37
7	54	54
8	111	289
9	184	136
10	15	121
11	1	14
14	0	66
15	0	10
16	0	19
18	0	13
24	0	1

Starting with Constellation A and networks comprising five OGSs, additional OGSs were incrementally included based on trade-off analysis results. The objective was to achieve a 99% availability for at least one target. The analysis revealed that a minimum of nine OGSs is required to meet this criterion. A total of 185 networks were tested, with the optimal network—achieving a weighted availability score of 0.984—comprising the following OGSs: Athens, Barcelona, Catania, Copenhagen, Marseille, Rome, Sevilla, Sofia, and Stockholm.

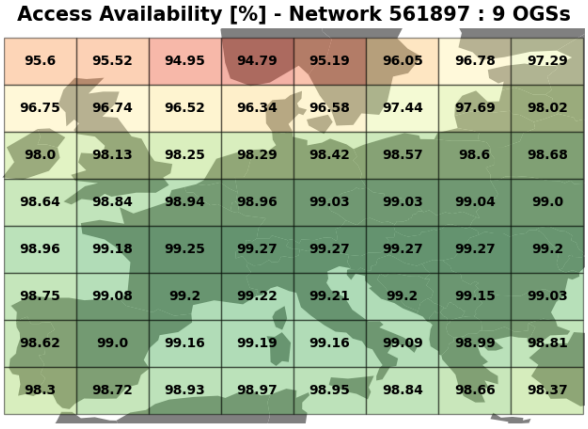

Fig. 13: Access availability for the optimal network of 9 OGSs for Constellation A.

While this network demonstrates strong performance at lower latitudes, important urban areas at

Table 6: Composition of the best networks tested per OGS number and Constellation.

OGS number	Network Composition
Constellation A	
5	Catania, Marseille, Sevilla, Sofia, Stockholm
6	Athens, Catania, Copenhagen, Marseille, Lisbon, Sevilla
7	Athens, Catania, Copenhagen, Marseille, Rome, Sevilla, Stockholm
8	Athens, Barcelona, Catania, Copenhagen, Marseille, Rome, Sevilla, Stockholm
9	Athens, Barcelona, Catania, Copenhagen, Marseille, Rome, Sevilla, Sofia, Stockholm
10	Athens, Barcelona, Catania, Copenhagen, Lisbon, Marseille, Rome, Sevilla, Sofia, Stockholm
Constellation B	
5	Barcelona, Catania, Copenhagen, Marseille, Sofia
6	Barcelona, Catania, Copenhagen, Marseille, Rome, Sofia
7	Athens, Barcelona, Catania, Copenhagen, Marseille, Rome, Sofia
8	Athens, Barcelona, Catania, Copenhagen, Marseille, Porto, Rome, Sofia
9	Athens, Barcelona, Catania, Copenhagen, Marseille, Porto, Rome, Sofia, Stockholm
10	Athens, Barcelona, Catania, Copenhagen, Marseille, Porto, Rome, Sofia, Stockholm, Vienna

higher latitudes still exhibit lower availability scores, necessitating an increase in the number of OGSs. Further analysis determined that an optimal network configuration requires 11 OGSs to achieve superior performance. Following the identification of the best 9-OGS network, the trade-off analysis script was employed to suggest configurations for 10 and subsequently 11 OGSs. The optimal 11-OGS network comprises the following OGSs: Athens, Barcelona, Catania, Copenhagen, Marseille, Paris, Rome, Sevilla, Sofia, Stockholm, and Warsaw. The access availability plot for this network is presented in figure 14.

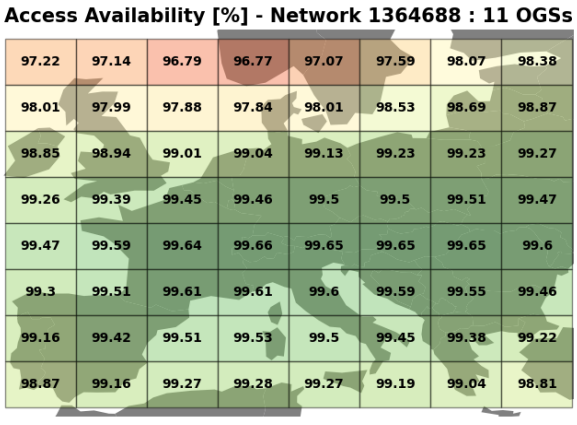

Fig. 14: Access availability for the optimal network of 11 OGSs for Constellation A.

With this network configuration, all major targets achieve availability values exceeding 99%, extending up to nearly 99.7%. Consequently, further analysis for Constellation A with OISL was deemed unnecessary, as the marginal benefits of adding more OGSs do not justify the increased costs and infrastructure complexity. The same process was applied to Constellation B using the OISL chain databases, aiming to identify whether high-performing networks from Constellation A would show similar characteristics, while anticipating some differences. Starting with 5 OGSs, the previously best network—the Southern network—had an availability score of 0.84. After testing 380 networks, the best configuration emerged as Barcelona, Catania, Copenhagen, Marseille, and Sofia, achieving a score of 0.848. With a focus on improving the availability score, networks with increasing numbers of OGSs were tested up to a total of 16. It became evident that for Constellation B, 11 OGSs were insufficient to reach a 99% availability, contrary to the findings for Constellation A. Consequently, 66 networks with 14 OGSs and 19 networks with 16 OGSs were tested. The best network of 16 OGSs, shown in figure 15(a), achieved a weighted score of 0.9753, inferior to the one of 0.984 for the best network of 9 OGSs in Constellation A. Given that, an analysis was conducted using all 24 OGSs to understand the upper performance limit. This test, depicted in figure 15(b), is hypothetical due to the unfeasibility of deploying 24 OGSs in terms of cost and mission complexity. However, it provides crucial insights for subsequent trade-off analyses. The weighted availability score for this extensive network was 0.9857, which still falls short of the best 11 OGS network of Constellation A, which scored 0.991. These findings indicate that increasing the number of OGSs in Constellation B does not

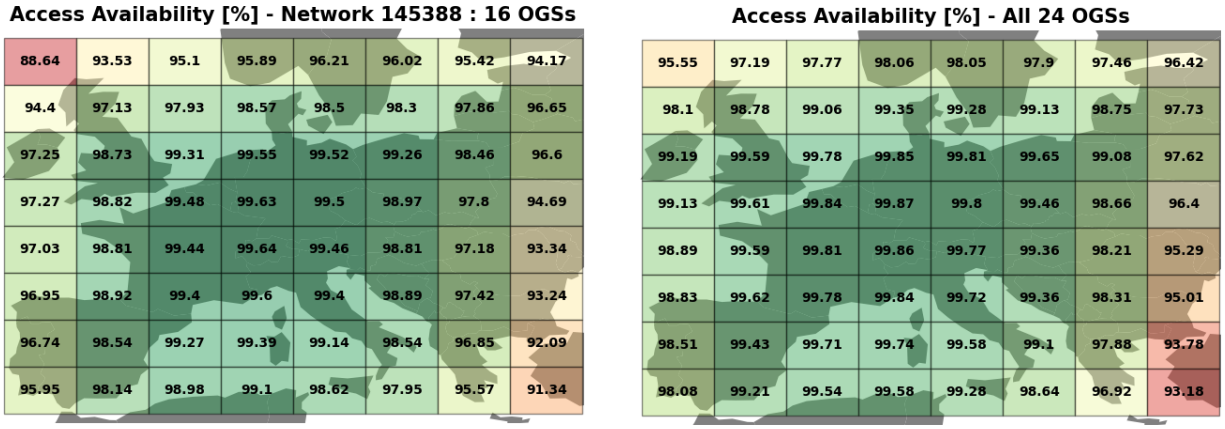

(a) Access availability for the best network of 16 OGSs for Constellation B.

(b) Access availability for Constellation B considering all 24 OGSs.

Fig. 15: Access Availability maps for constellation B, with FHO and OISL.

yield the same level of performance improvement as observed in Constellation A, highlighting the complexity and challenges inherent in optimizing OGS networks for different constellations. These analyses allowed us to draw several important conclusions. Firstly, the performance of Constellation B is significantly lower than that of Constellation A. For Constellation A, an operable network with high performance can be achieved with 11 OGSs. In contrast, even considering the upper limit of 24 OGSs for Constellation B, the performance remains inferior, coupled with higher capital and operational costs and increased mission complexity. Secondly, the introduction of OISL and the resulting improvement in coverage show that the most effective networks predominantly have their OGSs located in southern Europe, with Catania, Marseille, Sofia, and Athens featuring in nearly all top-performing networks. This geographical trend is mostly attributed to the superior weather conditions in southern Europe compared to those of northern Europe. Furthermore, the trade-off tool's strategy to prioritize OGSs that can minimize overall outage time due to cloud blockage has proven effective. The top-performing networks identified through a less filtered combination test largely coincide with those suggested by the tool, and in cases where they differ, their performance is nearly identical. Additionally, the increase in access availability does not scale linearly with the number of OGSs added. The addition of an OGS is considerably more beneficial when the total number of OGSs is lower, compared to when the network already has a substantial number of OGSs. Finally, the best-performing networks can readily achieve availabilities of 99% at lower and middle latitudes. However, they struggle at higher latitudes, where the uppermost targets exhibit significantly lower availabilities compared to their southern counterparts. This disparity is again due to the geographical and topological biases mentioned earlier.

5 Conclusions

In the present paper, an analysis of the E2E availability was presented for two satellite constellations concepts. The impact of cloud blockage and OISLs for the E2E availability between the OGS Network and targets across the European area was assessed. At first, different groups of 5 OGSs each were selected to investigate the availabilities achievable. It was determined that an OGS Network of this size is not sufficient to comply with a 99%+ availability across the European targets, due to both topological and cloud-blockage limitations, even when OISL is implemented. The following step was to increase the size of the OGS Network. A Network Optimisation routine was developed, taking into account the cloud-free availability, prioritisation of highly populated targets, and location distance for weather decorrelation.
This tool allowed to assess that for Constellation A (higher LEO, low density), with OISL enabled, a specific group of 11 OGSs would perform well enough to obtain an E2E availability above 99% for the vast majority of the targets. On the contrary, for Constellation B (lower LEO, high density), still with OISL enabled, much larger OGS networks were required

to to obtain comparable results. As stated in Section 4, weighted availability of Constellation B with all 24 OGSs enabled would reach 0.986, lower than what Constellation A achieves with only 11 OGSs (0.991). Constellation A amplifies the geographical decoupling provided when favouring southern locations for the OGS distribution and serving higher latitude targets. This is due to the larger swath and coverage persistence given by the higher altitude of the satellites, and the extended range of the OISLs. Future works might consider the implementation of more dynamic OISL topologies, allowing for selection of satellite nodes that have better availability of high priority targets. This would allow to further increase the availability or decrease the number of OGSs required to achieve a certain availability requirement.

Acronyms

Optical Satellite Links (OSL)
Optical Ground Stations (OGS)
Optical Inter-Satellite Links (OISL)
End-to-End (E2E)
Free Space Optical Communications (FSOC)
Network Optimisation (NO)
Optical Groung-to-Space Link (OGSL)
AGI System Tool Kit (STK)
Feederlink HandOver (FHO)

Aknowledgements

The authors would like to acknowledge the discussions and the financial support of the European Space Agency (ESA) under the Project "Feeder Link Architectures for Future NGSO Constellations", Contract No. ESA AO/1-11080/21/UK/ND. The views of the authors do not reflect the views of the Agency.

References

[1] Hemani Kaushal and Georges Kaddoum. "Optical Communication in Space: Challenges and Mitigation Techniques". In: *IEEE Communications Surveys and Tutorials* 19 (2017), pp. 57–96. URL: https://api.semanticscholar.org/CorpusID:19239549.

[2] D. L. Fried. "Optical Resolution Through a Randomly Inhomogeneous Medium for Very Long and Very Short Exposures". In: *Journal of the Optical Society of America* 56 (1967), pp. 1372–1379. URL: http://ui.adsabs.harvard.edu/abs/1966JOSA...56.1372F/abstract.

[3] Keith E. Wilson and James R. Lesh. "An Overview of the Galileo Optical Experiment (GOPEX)". In: *Communications Systems Research Section* (1993). URL: https://www.semanticscholar.org/paper/An-Overview-of-the-Galileo-Optical-Experiment-Wilson-Lesh.

[4] Keith E. Wilson et al. "Overview of the Ground-to-Orbit Lasercom Demonstration (GOLD)". In: *Photonics West*. National Institute of Information and Communications Technology. 1997. URL: https://api.semanticscholar.org/CorpusID:33883421.

[5] Keith E. Wilson. "An Overview of the GOLD Experiment Between the ETS-6 Satellite and the Table Mountain Facility". In: Communications Systems and Research Section. 1996. URL: https://api.semanticscholar.org/CorpusID:129678662.

[6] Toni Tolker-Nielsen and Gotthard Oppenhauser. "In-orbit test result of an operational optical intersatellite link between ARTEMIS and SPOT4, SILEX". In: *SPIE LASE*. European Space Agency/ESTEC, France). 2002. URL: https://api.semanticscholar.org/CorpusID:61414144.

[7] David J. Israel et al. "Early results from NASA's laser communications relay demonstration (LCRD) experiment program". In: *SPIE*. 2023. URL: https://www.spiedigitallibrary.org/conference-proceedings-of-spie/11536/1153619/Early-results-from-NASAs-laser-communications-relay/10.1117/12.2655481.short.

[8] European Space Agency. *European Data Relay Satellite System (EDRS) Overview*. Visited on 12/07/2023. 2023. URL: https://connectivity.esa.int/european-data-relay-satellite-system-edrs-overview.

[9] Nils Pachler et al. "An Updated Comparison of Four Low Earth Orbit Satellite Constellation Systems to Provide Global Broadband". In: *2021 IEEE International Conference on Communications Workshops (ICC Workshops)*. 2021, pp. 1–7. DOI: 10.1109/ICCWorkshops50388.2021.9473799.

[10] DCP. *Colt Fibre Map*. https://dcp.colt.net/coltFibreMapv2/?lang=en. URL: https://dcp.colt.net/coltFibreMapv2/?lang=en (visited on 09/18/2024).

[11] Christian Fuchs et al. "Optimization and throughput estimation of optical ground Networks for LEO-downlinks, GEO-feeder links and GEO-relays". In: DLR. Feb. 2017, p. 1009612. DOI: 10.1117/12.2254795.